AFRL-VA-WP-TP-2006-342

DYNAMIC COUPLING OF THE KC-135 TANKER AND BOOM FOR MODELING AND SIMULATION (POSTPRINT)

Austin L. Smith and Donald L. Kunz

AUGUST 2006

Approved for public release; distribution is unlimited.

STINFO COPY

AIR VEHICLES DIRECTORATE
AIR FORCE MATERIEL COMMAND
AIR FORCE RESEARCH LABORATORY
WRIGHT-PATTERSON AIR FORCE BASE, OH 45433-7542

NOTICE AND SIGNATURE PAGE

AFRL-VA-WP-TP-2006-342 HAS BEEN REVIEWED AND IS APPROVED FOR PUBLICATION IN ACCORDANCE WITH ASSIGNED DISTRIBUTION STATEMENT.

*//Signature//

Austin L. Smith
Associate Aerospace Engineer

//Signature//

GARY K. HELLMANN, Chief
Aerospace Vehicles Technology
Assessment & Simulation Branch

//Signature//

JEFFREY C. TROMP
Senior Technical Advisor
Control Sciences Division
Air Vehicles Directorate

This report is published in the interest of scientific and technical information exchange, and its publication does not constitute the Government's approval or disapproval of its ideas or findings.

*Disseminated copies will show "//Signature//" stamped or typed above the signature blocks.

REPORT DOCUMENTATION PAGE

Form Approved
OMB No. 0704-0188

1. REPORT DATE *(DD-MM-YY)*	2. REPORT TYPE	3. DATES COVERED *(From - To)*
August 2006	Conference Paper Postprint	01/01/2006 – 08/01/2006

4. TITLE AND SUBTITLE
DYNAMIC COUPLING OF THE KC-135 TANKER AND BOOM FOR MODELING AND SIMULATION (POSTPRINT)

5a. CONTRACT NUMBER
In-house

5b. GRANT NUMBER

5c. PROGRAM ELEMENT NUMBER
62201F

6. AUTHOR(S)
Austin L. Smith (AFRL/VACD)
Donald L. Kunz (AFIT/ENY)

5d. PROJECT NUMBER
2403

5e. TASK NUMBER
01

5f. WORK UNIT NUMBER
5Y

7. PERFORMING ORGANIZATION NAME(S) AND ADDRESS(ES)

Assessment & Simulation Branch (AFRL/VACD)
Control Sciences Division
Air Vehicles Directorate
Air Force Materiel Command, Air Force Research Laboratory
Wright-Patterson Air Force Base, OH 45433-7542

Engineering and Management (AFIT/ENY)
Air Force Institute of Technology
Wright-Patterson AFB, OH 45433

8. PERFORMING ORGANIZATION REPORT NUMBER
AFRL-VA-WP-TP-2006-342

9. SPONSORING/MONITORING AGENCY NAME(S) AND ADDRESS(ES)

Air Vehicles Directorate
Air Force Research Laboratory
Air Force Materiel Command
Wright-Patterson Air Force Base, OH 45433-7542

10. SPONSORING/MONITORING AGENCY ACRONYM(S)
AFRL-VA-WP

11. SPONSORING/MONITORING AGENCY REPORT NUMBER(S)
AFRL-VA-WP-TP-2006-342

12. DISTRIBUTION/AVAILABILITY STATEMENT
Approved for public release; distribution is unlimited.

13. SUPPLEMENTARY NOTES
This is a work of the U.S. Government and is not subject to copyright protection in the United States.

Conference paper published in the Proceedings of the 2006 AIAA Modeling and Simulation Technologies Conference and Exhibit published by AIAA. PAO Case Number: AFRL/WS 06-1818 (cleared July 26, 2006). Paper contains color.

14. ABSTRACT

Current Automated Aerial Refueling (AAR) research requires precision modeling and simulation of the refueling process between a KC-135 tanker aircraft and an unmanned aircraft. In order to meet this requirement, both steady-state and dynamic interactions between the tanker aircraft, the refueling boom, and the receiver aircraft must be accurately represented. Boom orientation and motion is known to change the trim of the tanker aircraft, which in turn influences the formation flying and station keeping tasks involved in current Air Force AAR concepts of operation. This paper describes the development of the coupled equations of motion for the refueling boom, which model its motion and its dynamic interactions with the tanker. For the purposes of this investigation, and to validate the boom model dynamics, the coupled boom model is first implemented as a boom-only simulation. The coupled model is compared to two existing boom-only models: one of which has been used for aerial refueling improvement studies, and the other is currently being used for boom operator training. Steady-state and dynamic responses to control inputs to the boom are calculated by the coupled boom model, then compared to those calculated using the existing models.

15. SUBJECT TERMS
KC-135, Refueling Boom, aerial refueling, multi-body dynamics, modeling, simulation

16. SECURITY CLASSIFICATION OF:			17. LIMITATION OF ABSTRACT:	18. NUMBER OF PAGES	19a. NAME OF RESPONSIBLE PERSON (Monitor)
a. REPORT	b. ABSTRACT	c. THIS PAGE			Austin L. Smith
Unclassified	Unclassified	Unclassified	SAR	20	19b. TELEPHONE NUMBER *(Include Area Code)* N/A

Standard Form 298 (Rev. 8-98)
Prescribed by ANSI Std. Z39-18

Dynamic Coupling of the KC-135 Tanker and Boom for Modeling and Simulation

Austin L. Smith*
Air Force Research Laboratory, Wright Patterson AFB, OH, 45433

and

Donald L. Kunz†
Air Force Institute of Technology, Wright Patterson AFB, OH, 45433

Current Automated Aerial Refueling (AAR) research requires precision modeling and simulation of the refueling process between a KC-135 tanker aircraft and an unmanned aircraft. In order to meet this requirement, both steady-state and dynamic interactions between the tanker aircraft, the refueling boom, and the receiver aircraft must be accurately represented. Boom orientation and motion is known to change the trim of the tanker aircraft, which in turn influences the formation flying and station keeping tasks involved in current Air Force AAR concepts of operation. This paper describes the development of the coupled equations of motion for the refueling boom, which model its motion and its dynamic interactions with the tanker. For the purposes of this investigation, and to validate the boom model dynamics, the coupled boom model is first implemented as a boom-only simulation. The coupled model is compared to two existing boom-only models: one of which has been used for aerial refueling improvement studies, and the other is currently being used for boom operator training. Steady-state and dynamic responses to control inputs to the boom are calculated by the coupled boom model, then compared to those calculated using the existing models.

Nomenclature

A	=	direction cosine transformation matrix
B	=	velocity transformation matrix
C_D	=	ruddevator cross section drag coefficient
C_L	=	ruddevator cross section lift coefficient
c	=	ruddevator cross section chord
D	=	Jacobian of the vector of constraint equations
F	=	aerodynamic force vector, or floating joint velocity transformation block matrix
I	=	inertia/mass matrix
M	=	aerodynamic moment vector
m	=	mass
n	=	unit vector
P	=	prismatic joint velocity transformation block matrix
p	=	generalized velocity vector
Q	=	generalized force/moment vector
q	=	generalized displacement vector
r	=	position vector
U	=	universal joint velocity transformation block matrix
u_E	=	displacement of the boom extension (positive extending)
V_x	=	ruddevator cross section velocity in the x direction
V_y	=	ruddevator cross section velocity in the y direction

* Associate Aerospace Engineer, Air Vehicles Directorate, Member AIAA
† Associate Professor, Department of Aeronautics & Astronautics, Associate Fellow AIAA

V_z = ruddevator cross section velocity in the *z* direction
v = velocity vector
α = ruddevator cross section angle of attack
Δ = identity matrix
η = vector of joint coordinates
θ = ruddevator pitch angle
λ = vector of Lagrange multipliers
ρ = air density
Φ = vector of constraint equations
ϕ = ruddevator cross section flow angle
ψ = ruddevator cross section yawed flow correction
ω = angular velocity vector

Subscripts and superscripts
B = tanker
E = boom extension
F = fixed boom
I = inertial space
R = ruddevator
θ = fixed boom pitch
ψ = fixed boom yaw
S = system

Operators
$\dot{(\,)}$ = derivative with respect to time
$\tilde{(\,)}$ = skew-symmetric matrix[1] defined such that $\tilde{a}^T = -\tilde{a}$

I. Introduction

Future Unmanned Aerial Vehicle (UAV) missions will include overseas and long-range flights which require aerial refueling. Refueling UAVs en-route introduces new issues not encountered in manned aircraft aerial refueling operations. In order to address these issues and to train personnel involved in the refueling process, advanced, high-fidelity models and simulations are necessary. High-fidelity, analytical models of the KC-135 tanker, shown in Fig. 1, the refueling boom, and the UAVs currently exist separately, but no existing single system models the dynamic interactions between them. In order to improve the modeling of automated aerial refueling and accurately simulate the refueling process, the dynamic interactions of the three bodies must be integrated. This paper will specifically address the tanker-boom interactions, and how to model them for simulation purposes.

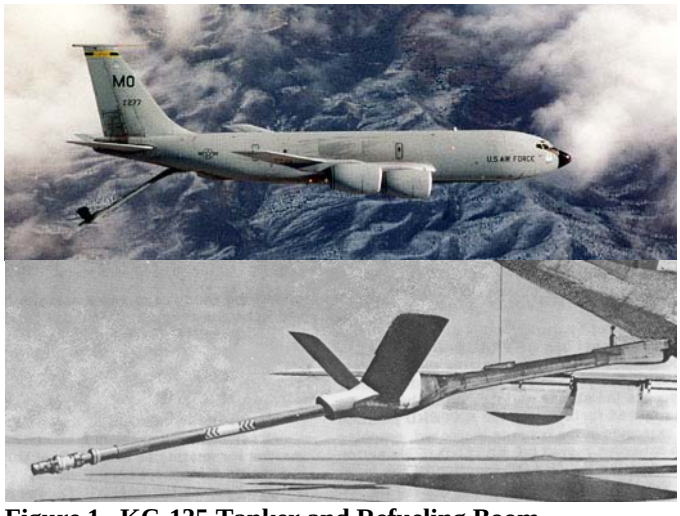

Figure 1. KC-135 Tanker and Refueling Boom.

The KC-135 aerial refueling boom is attached to the aircraft at the boom root by a vertical pin and a yoke and trunnion assembly, a combination known as the boom fork shown in Fig. 2[2]. The pin, assumed to be aligned with the vertical aircraft axis, allows yawing movement and the yoke and trunnion assembly, attached to the pin, allows pitching movement. The fixed portion of the boom is attached to the boom fork and extends 27 feet eight inches, and ends in an enlarged fairing to which two control surfaces, called ruddevators, are attached. The ruddevators each have a 31 inch chord, a 61 inch span, and are mounted at a 42 degree dihedral

angle. They allow the boom operator to fly the boom to the receiver aircraft's receptacle and also help to alleviate loads on the boom and bending during connected flight. A mechanical pantograph system positions the ruddevators nearly parallel to the airstream, a process known as auto-rotation, keeping them at low angles of attack and alleviating air loads on the boom without input from the boom operator. This is accomplished by rotating them as a function of boom yaw and pitch. An extendable portion of the boom, 27 feet long, retracts completely inside the fixed boom, and extends up to 20 feet outside the fixed boom. The boom extension ends in a nozzle for fuel transfer. The boom operator further deflects the ruddevators and extends or retracts the boom using two control levers in the boom operator station, a compartment forward of the boom fork on the underside of the KC-135.

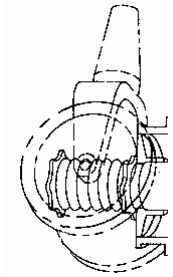

Figure 2. Boom Fork

II. Existing Models

The current analytical models used for simulating automated aerial refueling at the Air Force Research Laboratory (AFRL) consist of a high-fidelity Boeing KC-135 model and the Boom Operator Part Task Trainer (BOPTT) boom model, a model developed for the Air Education and Training Command and used in a boom operator training simulator. The boom model is attached geometrically to the tanker at the boom root and behaves as though it were translating through the air on an imaginary rigid rail at the attachment point. The BOPTT equations of motion (EOMs) and aerodynamic build-up, as they are implemented into the AFRL simulation, do not allow for dynamic interactions with the tanker aircraft. Similarly, the tanker model is not affected by any boom dynamics or aerodynamics. Since it is well known that the boom position and motion can change the trim of the tanker aircraft in free flight, a new, integrated model must be developed. This new analytical model incorporates aircraft motion effects into the boom dynamics and aerodynamics; and the boom forces and moments should in turn be transmitted to the tanker.

Because the BOPTT model is used for boom operator training and has been evaluated by boom operators at AFRL, the uncoupled dynamic responses of the BOPTT are used to validate the new boom model dynamics after its development. BOPTT aerodynamic equations are dependent on Mach number, so a large range of flight conditions varying altitude and Mach number can be examined. However, BOPTT aerodynamic and gravitational terms are directly applied to moment equations and do not straightforwardly provide forces, which are necessary for a coupled model. At AFRL, the BOPTT model is written in C, but to simplify it for development and testing, the EOMs and aerodynamic model were rewritten in MATLAB®, and placed in an S-function for use in a Simulink® model[3]. The Simulink® model provides an environment for rapid comparisons of boom motion as the new dynamically coupled model is developed. Different control stick movements can be commanded, and the resultant dynamic response of the boom can be observed.

Another existing boom model was developed at the Air Force Institute of Technology (AFIT), and used for research on how to increase the operational capability of the boom with today's new receiver aircraft. This model, like the BOPTT model, does not take into account coupling effects with the tanker, but does include pertinent physical characteristics and information needed for the new model's development, such as boom and ruddevator dimensions, boom component weights, and ruddevator airfoil information. The dynamic simulation using this model focused on ideal refueling conditions, and assumed a fixed boom extension for each simulation run. Consequently, the model was modified to include boom extension and retraction during a simulation. Aerodynamic and gravitational forces in the AFIT model are evaluated for individual components of the boom, then multiplied by a moment arm and summed to find the resultant moment, a similar approach to the coupled model. This model was converted to MATLAB® and placed in the simulation containing the BOPTT, expanding the test environment for analysis and synthesis of multiple boom models that can be simultaneously executed and compared in short order.

Although the existing models will be used for defining specific KC-135 refueling boom features and for verification of the new model's responses to control inputs, both the BOPTT and AFIT models have embedded simplifications and assumptions which were appropriate for their respective purposes, but do not meet the requirements of a full, coupled model needed for automated aerial refueling research. Hence, the new model was generated using a mechanical multi-body system analysis method and a new aerodynamic model.

III. Coupled Tanker/Refueling Boom Analytical Model

There are a number of methods that can be used to derive the equations of motion for an analytical model of the tanker/refueling boom system. The rationale for choosing the method described below was driven by the desire to ensure as much compatibility as possible between this model and an existing Simulink® model of the KC-135 tanker. Future research plans call for integrating the present model and the Simulink® tanker model.

The equations of motion for the Simulink® KC-135 tanker model are written in the form shown in Eq. (1), where the tanker is modeled as a rigid body, and the aerodynamic force and moment vectors on the right-hand side of Eq. (1) are functions of the aircraft states (velocities and displacements) and the pilot control inputs.

$$\begin{bmatrix} m_B\Delta & 0 \\ 0 & I_B \end{bmatrix} \begin{Bmatrix} \dot{v}_B \\ \dot{\omega}_B \end{Bmatrix} = \begin{Bmatrix} F_B \\ M_B - \tilde{\omega}_B I_B \omega_B \end{Bmatrix} \tag{1}$$

Simulink® solves Eq. (1) by first calculating the aircraft accelerations by multiplying both sides by the inverse of the aircraft inertia matrix. Then, the accelerations are integrated to get the velocities, which are in turn integrated to get the aircraft displacements. Prior to the second integration, the angular velocities must be transformed to aircraft attitude rates. Given this formulation and solution of the equations of motion for the tanker alone, a compatible form of the equations of motion for the coupled tanker/boom system is desired.

Therefore, in the present model, the equations of motion for the tanker are written exactly as shown in Eq. (1). The origin of the tanker coordinate system is located at the mass center of the aircraft, and the axes correspond to the standard aircraft coordinate system (*x* positive forward, *y* positive to starboard, *z* positive down).

The method chosen for formulating and solving the equations of motion for the refueling boom and coupling them to the tanker equations employs an implementation of joint coordinates and the velocity transformation[4,5]. This method permits the independent derivation of the equations of motion for each body in the system. Those equations are subsequently coupled to one another to form a system of equations in a form analogous to that shown in Eq. (1).

A. Refueling Boom

The refueling boom is modeled as two rigid bodies, a fixed boom and a boom extension, which are connected to one another. The fixed boom is fixed only in the sense that one end is attached to the tanker fuselage at the boom pivot, about which the fixed boom is permitted to yaw and pitch relative to the fuselage. Control of the fixed boom is facilitated by two ruddevators, which are attached to the fixed boom near its free end. The ruddevators are also modeled as rigid bodies, each of which is controlled in pitch about its axis of aerodynamic centers. The boom extension telescopes out of the fixed boom along an axis parallel to the longitudinal axes of the fixed boom and boom extension.

1. Fixed Boom

The origin of the fixed boom coordinate system is located at the boom pivot, not at its mass center. The axes of the fixed boom coordinate system are defined such that when the boom yaw and pitch angles are zero, the boom axes are aligned with the tanker axes. Therefore, the *x* axis points in the direction of the boom pivot when viewed from the boom tip, the boom pitches about the *y* axis, and the *z* axis nominally points down.

Mass and inertia properties for the fixed boom were derived from, but are not identical to the mass and inertia properties described in Ref. 2, since the author models the entire refueling boom as a single body with variable mass and inertia properties. Using the weight breakdown contained in Ref. 2, the weights of the fixed boom components are listed in Table 1. Moments of inertia for the fixed boom are calculated assuming that fixed masses are point masses and that distributed masses are slender rods. Equation (2) contains the equations of motion for the fixed boom. Note that the form of Eq. (2) differs slightly from Eq. (1), in that the mass/inertia matrix in Eq. (2) includes off-diagonal block matrices and the force on the right-hand side includes an additional mass term. These additional terms appear because the origin of the fixed boom coordinate system is not located at the mass center of the fixed boom. The location of the mass center is indicated by an asterisk.

Items	Weight (lbm)	CG (in from pivot)
Snubber Hydraulic motor drive Stowage provisions Instrumentation Attaching provisions	122.5	0.0
Structure tube Fairing Hydraulics Fixed inner tube Electrical Fuel system	427.3 (distributed)	166.0
Ruddevators & supports Recoil assembly Ruddevator controls Ruddevator locking Dumping provisions	329.2	310.5

Table 1. Fixed Boom Weight Breakdown

$$\begin{bmatrix} m_F\Delta & -m_F\tilde{r}_{F^*/F} \\ m_F\tilde{r}_{F^*/F} & I_F \end{bmatrix} \begin{Bmatrix} \dot{v}_F \\ \dot{\omega}_F \end{Bmatrix} = \begin{Bmatrix} F_F - m_F\tilde{\omega}_F\tilde{\omega}_F r_{F^*/F} \\ M_F - \tilde{\omega}_F I_F \omega_F \end{Bmatrix} \tag{2}$$

On the right-hand side of Eq. (2) are force and moment terms due to gravity, aerodynamic drag, and aerodynamic forces on the ruddevators. Calculation of the forces and moments due to gravity are straightforward. The calculation of the aerodynamic drag on the fixed boom is not difficult, but a couple of issues must be addressed. First, the fixed boom fairing is not cylindrical, but rather is elliptical, to reduce the drag in the freestream direction. In addition, the fairing bulges significantly near the location of the ruddevators, and this also affects the drag calculation.

Forces and moments on the ruddevators are calculated from blade element theory. The origin of the coordinate system associated with each ruddevator is on the fixed boom centerline, where the pitch axis intersects it. Thus, the *x* axis for each ruddevator is oriented in the same direction as the fixed boom *x* axis, the *y* axis is collinear with the ruddevator pitch axis, and the *z* axis is nominally down. In order to account for the 42 degrees of dihedral for the ruddevators, the coordinate system for the left ruddevator is rotated 42 degrees about the *x* axis and the coordinate system for the right ruddevator is rotated -42 degrees. As a result of the rotation of the coordinate system for the left ruddevator, the positive direction of the *y* axis is inboard from the tip; while for the right ruddevator, the positive direction of the *y* axis is outboard toward the tip. Lift and drag forces are calculated at ruddevator cross sections, then integrated over the span of each ruddevator to obtain the forces and moments at the origin of the ruddevator coordinate systems.

$$F_R = \begin{Bmatrix} -\frac{1}{2}\rho c\int\left(V_x^2 + V_y^2 + V_z^2\right)C_D dy \\ 0 \\ -\frac{1}{2}\rho c\int\left(V_x^2 + V_y^2 + V_z^2\right)C_L dy \end{Bmatrix} \tag{3}$$

$$M_R = \begin{Bmatrix} -\frac{1}{2}\rho c\int\left(V_x^2 + V_y^2 + V_z^2\right)C_L y dy \\ 0 \\ \frac{1}{2}\rho c\int\left(V_x^2 + V_y^2 + V_z^2\right)C_D y dy \end{Bmatrix} \tag{4}$$

The lift and drag coefficients of the ruddevators' NACA 65_1-012 airfoil used in Eqs. (3) and (4) are interpolated from airfoil tables in which the coefficients are tabulated as functions of both angle of attack and Mach number. The angle of attack calculated at each cross section includes a correction for yawed flow, which is implemented as shown in Eqs. (5-7).

$$\psi = \frac{|V_x|}{\sqrt{V_x^2 + V_y^2}} \tag{5}$$

$$\phi = \tan^{-1}\left[\frac{V_z}{\mathrm{sgn}(V_x)\sqrt{V_x^2 + V_y^2}}\right] \tag{6}$$

$$\alpha = \tan^{-1}\left(\frac{\psi\sin\theta}{\cos\theta}\right) + \phi \tag{7}$$

Finally, the forces and moments for each ruddevator are transformed to act at and about the boom pivot, and are combined with the forces and moments due to gravity and aerodynamic drag. In this manner, a vector of forces and a vector of moments is constructed for use in Eq. (2).

2. Boom Extension

The origin of the boom extension coordinate system is located at the inboard end of the boom extension. The axes of the boom extension coordinate system are defined such that they are always aligned with the fixed boom axes. Therefore, the boom extension telescopes in the direction of the *x* axis.

Mass and inertia properties for the boom extension were also derived from the weight breakdown contained in Ref. 2, and are listed in Table 2. In addition to the items listed in Table 2, the fixed boom fills with fuel at the rate of 0.39 lbm/in as the boom is extended, replacing the volume vacated by the boom extension. Instead of bookkeeping the weight of this additional fuel with the fixed boom, it is included in the boom extension breakdown so that the properties of one body (fixed boom) are not dependent on the state of another body (boom extension). Therefore, the mass (m_E), mass center (r_E), and moments of inertia (I_E) of the boom extension are functions of its position relative to the boom pivot. Like the fixed boom, moments of inertia for the boom extension are calculated assuming that fixed masses are point masses and that distributed masses are slender rods. The resulting equations of motion for the boom extension are shown in Eq. (8). Equation (8) also includes the off-diagonal block matrices in the mass/inertia matrix and the additional mass term on the right-hand side, which result from the origin of the coordinate system not being located at the mass center.

Items	Weight (lbm)	CG (in from pivot)
Rollers & supports	23.4	u_E
Inner tube		
Tube lining	375.1	
Fuel	(distributed)	u_E + 165.0
Nozzle		
Shock absorber	62.0	u_E + 330.0

Table 2. Boom Extension Weight Breakdown

$$\begin{bmatrix} m_E\Delta & -m_E\tilde{r}_{E^*/E} \\ m_E\tilde{r}_{E^*/E} & I_E \end{bmatrix} \begin{Bmatrix} \dot{v}_E \\ \dot{\omega}_E \end{Bmatrix} = \begin{Bmatrix} F_E - m_E\tilde{\omega}_E\tilde{\omega}_E r_{E^*/E} \\ M_E - \tilde{\omega}_E I_E \omega_E \end{Bmatrix} \tag{8}$$

The force and moment terms on the right-hand side of Eq. (8) are due to gravity and aerodynamic drag. Calculation of the forces and moments due to gravity are straightforward, once the mass and center of mass for the boom extension are determined, based on its position. The aerodynamic drag calculation is slightly more complex than the drag calculation for the fixed boom, since the only portion of the boom extension that is subject to drag is that portion that extends beyond the fixed boom.

B. Coupled Tanker/Refueling Boom Equations of Motion

The uncoupled equations of motion for the tanker, fixed boom, and boom extension are combined into a single set of equations, as shown in Eq. (9).

$$\begin{bmatrix} m_B\Delta & 0 & 0 & 0 & 0 & 0 \\ 0 & I_B & 0 & 0 & 0 & 0 \\ 0 & 0 & m_F\Delta & -m_F\tilde{r}_F & 0 & 0 \\ 0 & 0 & m_F\tilde{r}_F & I_F & 0 & 0 \\ 0 & 0 & 0 & 0 & m_E\Delta & -m_E\tilde{r}_E \\ 0 & 0 & 0 & 0 & m_E\tilde{r}_E & I_E \end{bmatrix} \begin{Bmatrix} \dot{v}_B \\ \dot{\omega}_B \\ \dot{v}_F \\ \dot{\omega}_F \\ \dot{v}_E \\ \dot{\omega}_E \end{Bmatrix} = \begin{Bmatrix} F_B \\ M_B - \tilde{\omega}_B I_B \omega_B \\ F_F - m_F\tilde{\omega}_F\tilde{\omega}_F r_F \\ M_F - \tilde{\omega}_F I_F \omega_F \\ F_E - m_E\tilde{\omega}_E\tilde{\omega}_E r_E \\ M_E - \tilde{\omega}_E I_E \omega_E \end{Bmatrix} \tag{9}$$

In order to couple the independent equations for the tanker, fixed boom, and boom extension to one another, constraint equations must be derived for the joints that connect each of the three components. The boom pivot is essentially a universal joint (perpendicular yaw and pitch rotations) and, as such, generates four algebraic constraint equations. The telescopic motion of the boom extension relative to the fixed boom can be modeled as a prismatic joint, with five algebraic constraint equations. Using Lagrange multipliers, Eq. (9) can be combined with the nine constraint equations.

$$I_S \dot{p}_S - D^T \lambda = Q_S \tag{10}$$

$$\Phi\left(q_S\right) = 0 \tag{11}$$

where

$$\dot{\Phi}\left(q_S\right) \equiv Dp_S = 0 \tag{12}$$

At this point, the velocity transformation provides a means for expressing the generalized velocities of the system components in terms of the joint velocities.

$$p_S = B\dot{\eta} \tag{13}$$

Substitute Eq. (13) into Eq. (10) and multiply the resulting equation by the transpose of the velocity transformation matrix. The term containing the Lagrange multipliers is zero, based on the result of substituting Eq. (13) into Eq. (12). Then, the equations of motion for the coupled tanker/refueling boom system may be written in a form equivalent to that of Eq. (1).

$$B^T I_S B\ddot{\eta} = B^T\left(Q_S - I_S\dot{B}\dot{\eta}\right) \tag{14}$$

For integration with the Simulink® model of the KC-135 tanker, the equations of motion as shown in Eq. (14) is the preferred form, since it is similar to the form of the equations in the Simulink® model. However, for the simulations performed during this investigation, Eq. (14) was rewritten in first-order form, so that it would be compatible with the MATLAB® functions used to solve ordinary differential equations.

C. Velocity and Acceleration Transformations

In the previous section, the coupling between the tanker and fixed boom and between the fixed boom and boom extension was implemented using the velocity transformation matrix and its derivative, the acceleration transformation matrix. In general, the components of these matrices are dependent on the types of joints used in the mechanism, as well as the geometry of the mechanism. For this particular model, the tanker is a floating body (no constraint equations), the joint between the tanker and the fixed boom is a universal joint, and the joint between the fixed boom and the boom extension is a prismatic joint. The tanker/boom system takes the form of an open loop, single chain geometry with the sequence of joints described above. Therefore, the velocity transformation matrix takes the form shown in Eq. (15), where each of the components is a block matrix.

$$B = \begin{bmatrix} F_{BB} & 0 & 0 \\ F_{FB} & U_{FF} & 0 \\ F_{EB} & U_{EF} & P_{EE} \end{bmatrix} \tag{15}$$

The structure of the velocity transformation matrix in Eq. (15) reflects the topology (open chain, single branch) of the tanker/boom system. That is, the positions of the block matrices within the velocity transformation matrix are determined by the order in which the bodies are connected, and by the type of joint that connects the bodies. For example, the bottom row of the velocity transformation matrix (working right to left) indicates that the boom extension is connected to the fixed boom by a prismatic joint, the fixed boom is connected to the tanker by a universal joint, and the tanker is a floating body. By changing the block matrices in Eq. (15), one changes the kinematical connections between the bodies. For example, if the tanker was to be modeled as riding on a rail, then the entire first column of the velocity transformation matrix would consist of *P* block matrices, representing a prismatic joint.

The block matrices in Eq. (15) represent the kinematical connections between two bodies, which relate the uncoupled coordinates of each body to the joint coordinates. The dimensions of each block matrix are therefore determined by the type of joint it represents. Since the number of joint velocities in a floating joint is the same as the number of coordinates for an uncoupled rigid body, all of the *F* block matrices have six rows and six columns. Universal joints have two joint velocities, one for each rotation, so the *U* block matrices have six rows and two

columns. Only one joint velocity (translation) is needed for a prismatic joint and, therefore, the *P* block matrix has six rows and one column.

The structure of the block matrix for each type of joint can be predefined; although for this investigation, the block matrices were derived directly from the kinematics of the bodies, since the definition of the kinematics for the boom pivot differed slightly from the standard definition of a universal joint. The general forms of the block matrices for the floating, universal, and prismatic joints, as defined in this model, are shown in Eqs. (16)-(18), respectively

$$F_{XB} = \begin{bmatrix} A^{XI} & -A^{XB}\tilde{r}^{B}_{X/B} \\ 0 & A^{XB} \end{bmatrix} \tag{16}$$

$$U_{XF} = \begin{bmatrix} 0 & 0 \\ A^{XB}n^{B}_{\psi} & A^{XF}n^{F}_{\theta} \end{bmatrix} \tag{17}$$

$$P_{EE} = \begin{Bmatrix} n^{E}_{u} \\ 0 \end{Bmatrix} \tag{18}$$

IV. Coupled Model Testing and Evaluation

In order to compare the coupled model to the existing models in the Simulink® environment, the coupled model must be reverted back to an uncoupled model. Tanker interaction must be negated in order to compare the new model's control input responses to the existing uncoupled models. Aircraft translational motion is assumed to be only in the aircraft *x* axis direction, and all aircraft rotational terms are set to zero. Boom motion is now with respect to the boom fork traveling along the aircraft *x* axis at a given speed and altitude. After de-coupling the new model, it is placed in the multiple-boom simulation and subjected to the same inputs as the BOPTT and AFIT models.

For qualitative comparison purposes, hardware limits and the boom control system are neglected in order to compare unaltered equations of motion and aerodynamic characteristics and observe trends in boom motion. The boom control-stick position and ruddevator auto-rotation will be neglected to avoid any discrepancies in their implementation. Ruddevator deflections will be directly input into each model to ensure consistency between the model's initial conditions. Also, hardware limits such as maximum and minimum boom pitch and yaw angles due to the aircraft and boom structure and ruddevator deflection limits will be ignored. However, boom telescopic speed limits and extension position limits will be obeyed in order to compare changes in boom trim due to these movements. From Ref. 2, the nominal refueling position for the boom is at 30 degrees pitch down, zero degrees yaw, and 12.2 feet of extension. These tests use typical AAR simulation flight conditions at an aircraft forward velocity of 670 ft/s and an altitude of 25000 feet, using a standard atmosphere model. Test cases are simple step inputs of symmetric and asymmetric ruddevator deflections, in addition to their respective trim deflections, for pitch, yaw, and coupled pitch-yaw responses, dynamic trim changes due to boom extension, and sinusoidal motion due to sinusoidal inputs.

Although the BOPTT model is being used to validate the new model, AFIT model responses are also shown to demonstrate similar characteristics between it and the coupled model.

A. Symmetric Ruddevator Deflection from Trim

The first test case is a six degree step deflection of both the left and right ruddevators when the boom is trimmed at its nominal refueling configuration. From Fig. 3, it can be seen that the coupled model's response is more damped, has a higher frequency, and converges to a larger pitch angle than the BOPTT model. Differences in drag calculations on the boom and ruddevator control forces resulting from aerodynamic calculations account for differences in damping and the steady state equilibrium angle. BOPTT uses differential and cumulative ruddevator deflections and Mach dependent coefficients to calculate ruddevator moment contributions. The AFIT model uses a simple three-dimensional lift curve slope coefficient and the parabolic drag equation. Lastly, the coupled model uses the blade element theory discussed in Section III.A.1. Variations in mass distribution calculations may explain

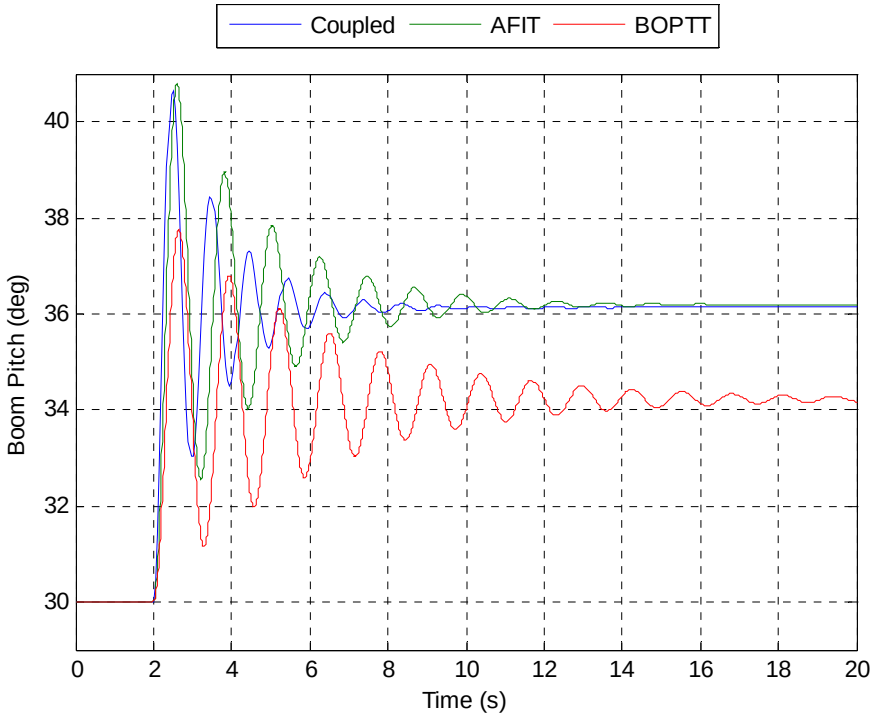

Figure 3. Boom Pitch Response to a Six Degree Symmetric Ruddevator Deflection.

discrepancies in the observed oscillation frequencies. Although Ref. 2 provides boom component weights, the exact distribution is unknown, and was approximated for the coupled model.

B. Asymmetric Ruddevator Deflection from Trim

A six degree step deflection of both ruddevators, but opposite in sign, was commanded when the boom was trimmed in its nominal configuration. From Fig. 4, the coupling effects of pitch motion due to yaw motion can be observed. The coupled model transient yaw response has less damping and a much higher frequency than the BOPTT model, and looks more like the AFIT model response. However, the steady state yaw angle of the coupled model is closer to that of the BOPTT than the AFIT model. The pitch coupling motion of the coupled model has a trend opposite to that of the BOPTT and AFIT models, though the BOPTT steady state pitch coupling angle is negligible. A yaw deflection causes a positive (down) relative deflection in pitch, whereas the BOPTT and AFIT models have a negative (up) relative deflection. Although drag on the boom will intuitively increase as yaw is increased, the ruddevator forces counteract this in the coupled model and force the boom down.

C. Trim Change due to Boom Extension, Starting from Nominal Condition

A step extension rate command was used to extend the boom from 12.2 feet to the maximum 20 feet extension starting with the boom trimmed at its nominal refueling configuration. The change in boom length and weight change the trim orientation of the boom, as seen in Fig. 5. The weight change is caused by additional fuel being added to the boom as it extends. The magnitude of the change in trim deflection for the coupled model is much larger, respectively, than either of the other models, but is in the same upward direction as the BOPTT model. Thus, the drag effects on the boom extension have more of an affect than the additional weight in the extension for the coupled model, and similarly in the BOPTT model. Conversely, the AFIT model shows more of an effect from the extension weight increase than its respective drag increase, moving the boom down.

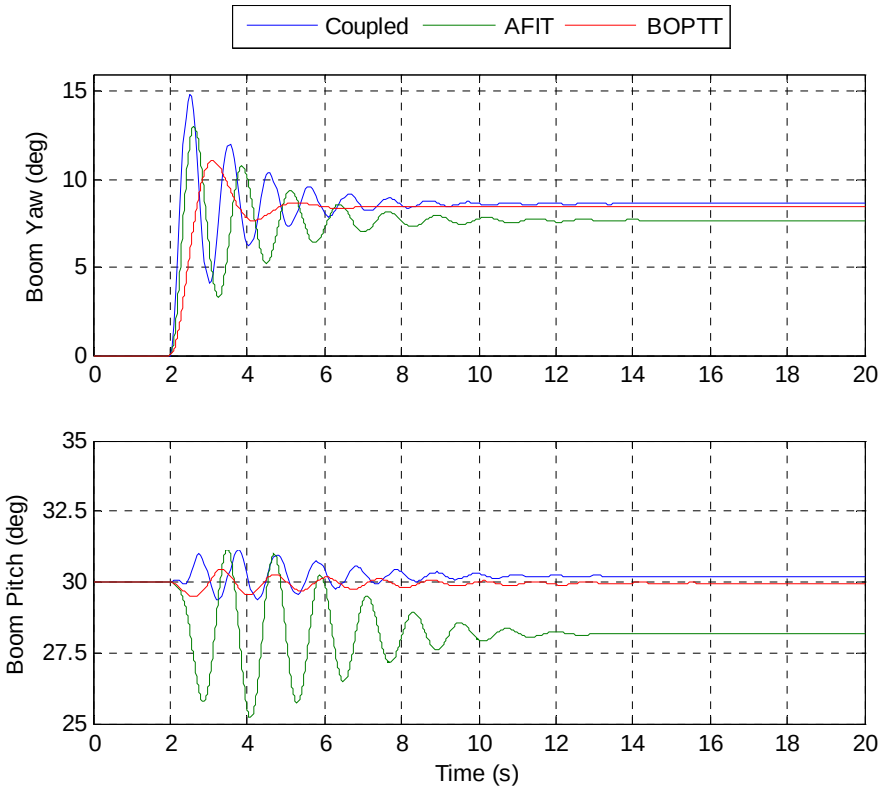

Figure 4. Boom Yaw and Pitch Responses to a Six Degree Asymmetric Ruddevator Deflection.

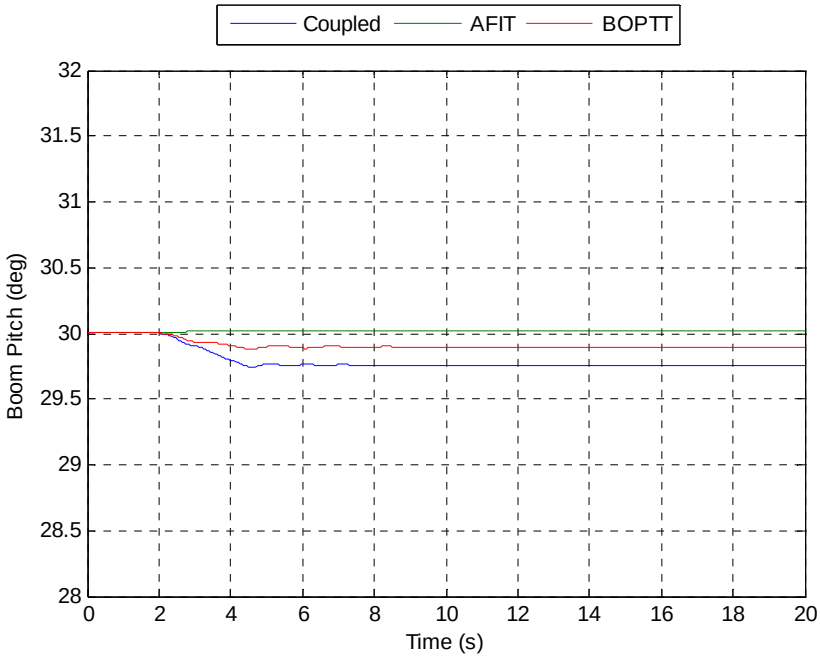

Figure 5. Boom Pitch Trim Change due to a Boom Maximum Extension from Nominal Refueling Orientation.

D. Trim Change due to Boom Extension, Starting from Abnormal Orientation

Another case was tested for trim changes due to boom extension and is shown in Fig. 6. For this case, the boom was trimmed at 30 degrees pitch, ten degrees yaw, and 12.2 feet extension, and then extended at its maximum rate to full extension. Pitch and yaw coupling effects can be observed in this test case, and all models show the same trends: a decrease in pitch angle, or movement upward, and a decrease in yaw angle towards center. The coupled model's yaw trim change due to this extension is relatively small when compared to the other two models. The wind velocity component in the boom extension y-axis direction does not produce a significant amount of drag, and therefore generates an insignificant yawing moment in the coupled model. Nevertheless, the differences in coupled model and BOPTT model deflections are trivial when compared to the magnitude of the trim deflections.

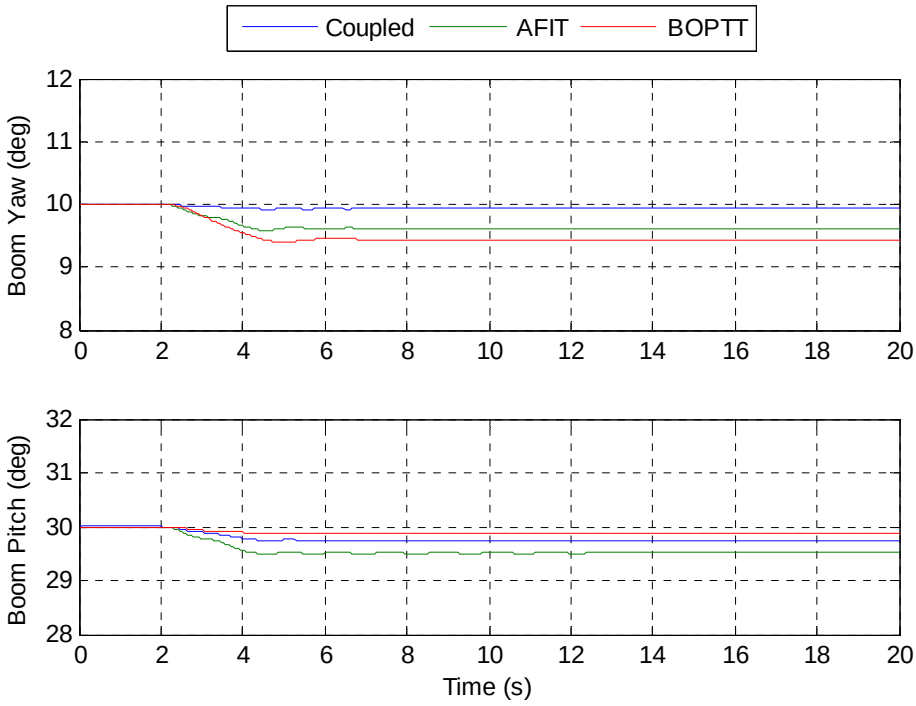

Figure 6. Boom Yaw and Pitch Trim Change due to a Boom Maximum Extension from a Yawed-Nominal Refueling Orientation.

E. Symmetric Sinusoidal Ruddevator Deflection from Trim

Symmetric sinusoidal ruddevator deflections, starting at trim and the boom initialized at its nominal position, were input into the models. The deflection magnitude is ten degrees relative to trim, with a frequency of 0.25 rad/s. The responses illustrated in Fig. 7 contain transient perturbations at the start of the simulation because the boom was trimmed at zero angular velocity, but converge to their steady state sinusoidal output after approximately ten seconds. It can be seen that the amplitudes of the boom pitch angles, for the coupled and AFIT models, are not symmetric about the trim orientation, even though the input sinusoid is. The deflection from trim is greater in the upward direction because, in addition to the ruddevator forces, the drag forces on the boom overcome its gravitational forces. The BOPTT model shows this same phenomenon, although it is much less evident, and the overall amplitude is considerably smaller.

F. Asymmetric Sinusoidal Ruddevator Deflection from Trim

Asymmetric sinusoidal ruddevator deflections, with the same initial conditions as in Section IV.E., were input into the models. The yaw response amplitudes, seen in Fig. 8, are symmetric about the trim orientation, except for transient perturbations caused by initial conditions. The BOPTT model contains an anomaly that prevents it from crossing zero yaw when the ruddevators are returned to their trim deflections. This is not seen in the coupled model,

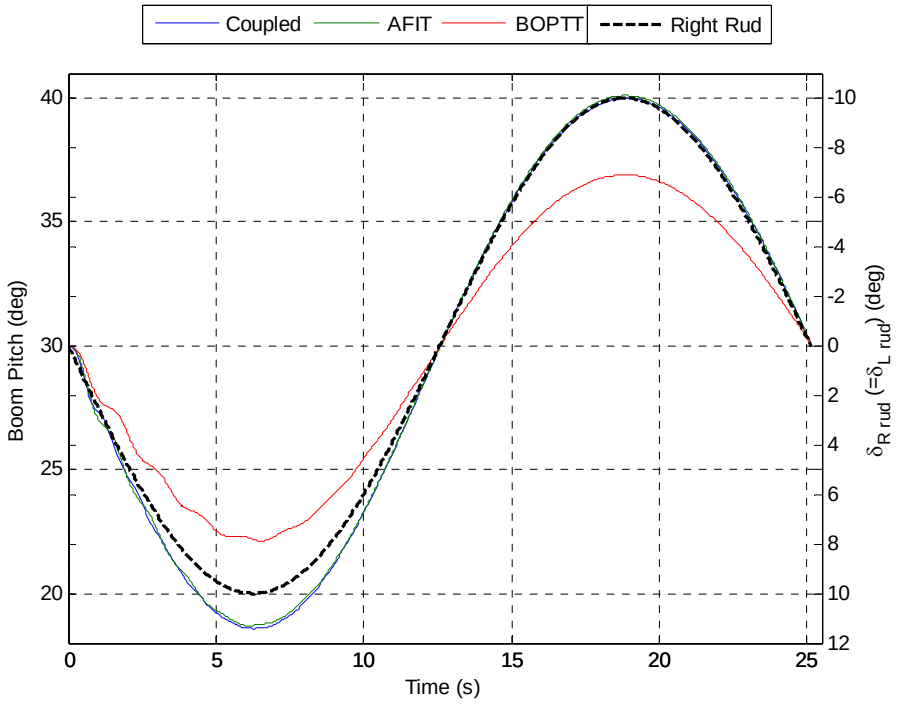

Figure 7. Boom Pitch Response to a Symmetric Sinusoidal Ruddevator Deflection.

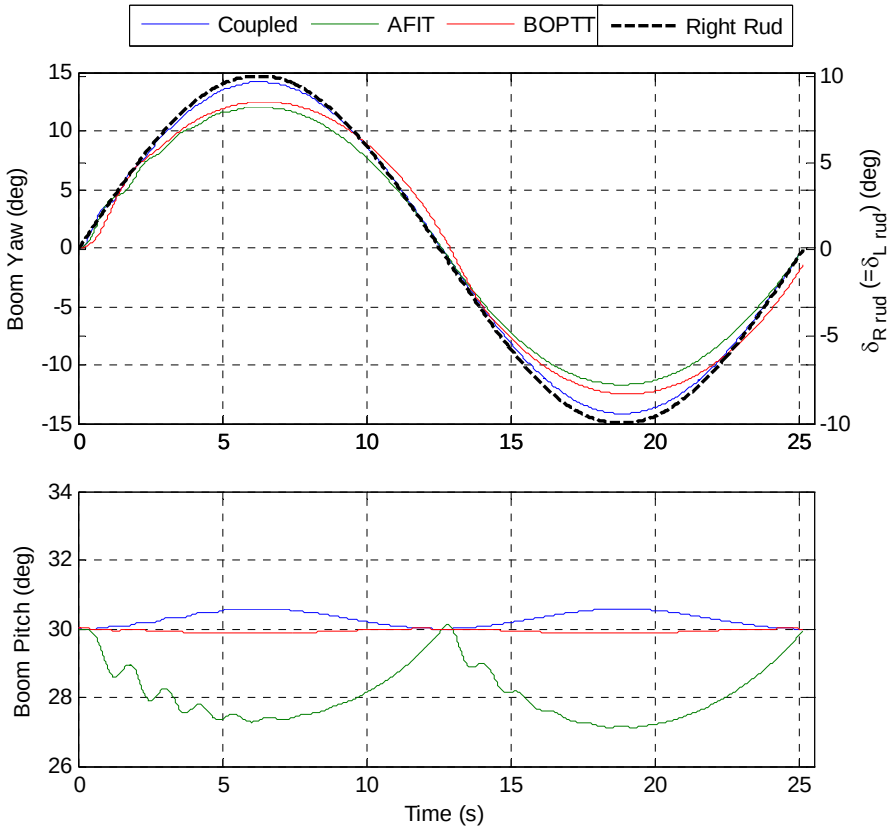

Figure 8. Boom Yaw and Pitch Response to a Asymmetric Sinusoidal Ruddevator Deflection.

or in the AFIT model, and could be caused by some irregular calculation in the BOPTT aerodynamics. The differences between the models in terms of yaw-pitch coupling are evident; pitch angle magnitude and direction both differ. These discrepancies can also be seen in Fig. 4, when they resulted from a step input. The coupled boom moves downward when displaced in yaw, whereas the AFIT moves upward and oscillates profoundly, and the BOPTT movement is also upward, but insignificant.

V. Conclusion

The coupled model responses, though not quantitatively equivalent to the BOPTT, are realistic and acceptable in terms of qualitative observations. Boom movement characteristics show the same basic trends between the two models, except in some yaw-pitch coupling instances. Even so, the discrepancies in yaw-pitch coupling between models will have little to no effect on the coupled tanker motion due to their small scale. The coupled model, based on first principles rather than empirical aerodynamics, can be improved upon with more information about the boom, such as its exact mass distribution. The coupled model dynamics will remain unchanged until further evaluations are done to assess its motion, such as integration with the tanker model and comparison with experimental data.

The coupled KC-135 boom model presented here will sufficiently provide similar responses to the BOPTT model while enabling coupling with the tanker aircraft. A more realistic interaction between the two dynamic bodies in AAR simulations is achievable without significantly changing the current simulation configuration that is based on input from boom operators and actual system hardware. Integration with the tanker model in Simulink®, and eventually its conversion into the AAR simulation environment are subsequent efforts to be carried out.

References

[1] Nikravesh, P.E., Computer-Aided Analysis of Mechanical Systems, Prentice-Hall, New Jersey, 1988, p. 25.

[2] Campbell, T.G. et. al., "System Study of the KC-135 Aerial Refueling System, Vol. I and II," M.S. Thesis, Department of Aeronautics and Astronautics, Air Force Institute of Technology, Wright Patterson AFB, OH, 1989.

[3] MATLAB® & Simulink® R2006a, The Mathworks, Inc., Natick, Massachusetts, 1984.

[4] Jerkovsky, W., "The Structure of Multibody Dynamics Equations," Journal of Guidance and Control, Vol. 1, No. 3, 1978, pp. 173-182.

[5] Kim, S.S. and Vanderploeg, M.L., "A General and Efficient Method for Dynamic Analysis of Mechanical Systems Using Velocity Transformation," ASME Journal of Mechanisms, Transmissions, and Automation in Design, Vol. 108, No. 2, 1986, pp. 176-182.